

# Toward Sustained Product Formation in the Liquid-Phase Hydrogenation of Mandelonitrile over a Pd/C Catalyst

Mairi I. McAllister, Cédric Boulho, Colin Brennan, Stewart F. Parker, and David Lennon\*

Cite This: *Org. Process Res. Dev.* 2020, 24, 1112–1123

Read Online

ACCESS |

Metrics & More

Article Recommendations

Supporting Information

**ABSTRACT:** The liquid-phase hydrogenation of the aromatic cyanohydrin mandelonitrile (MN,  $C_6H_5CH(OH)CN$ ) over a carbon-supported Pd catalyst to produce the primary amine phenethylamine (PEA,  $C_6H_5CH_2CH_2NH_2$ ) is investigated with respect to the transition from operation in single-batch mode to repeat-batch mode. While a single-batch reaction returns a complete mass balance, product analysis alongside mass balance measurements for a six-addition repeat-batch procedure shows an attenuation in the rate of product formation and an incomplete mass balance from the fourth addition onward. This scenario potentially hinders possible commercial operation of the phenethylamine synthesis process, so it is investigated further. With reference to a previously reported reaction scheme, the prospects of sustained catalytic performance are examined in terms of acid concentration, stirrer agitation rate, catalyst mass, and hydrogen availability. Gas–liquid mass transfer coefficient measurements indicate efficient gas  $\rightarrow$  liquid transfer kinetics within the experimental constraints of the Henry's law limitation on hydrogen solubility in the process solvent (methanol). Deviations from the optimized product selectivity are attributed to mass transport constraints, specifically the  $H_2(\text{sol}) \rightarrow 2H(\text{ads})$  transition, which is ultimately restrained by the availability of  $H_2(\text{sol})$ . Finally, in an attempt to better understand the deactivation pathways, inelastic neutron scattering measurements on a comparable industrial-grade catalyst operated in an analogous reaction in fed-batch mode indicate the presence of an oligomeric overlayer postreaction. This overlayer is thought to be formed via oligomerization of hydroxyimine or imine species via specific pathways that are identified within a postulated global reaction scheme.

**KEYWORDS:** selective hydrogenation, mandelonitrile, Pd/C, phenethylamine, process optimization

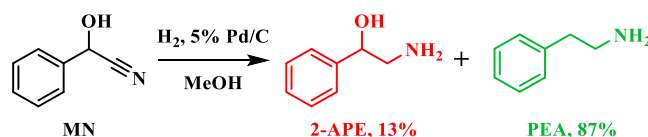
## 1. INTRODUCTION

Primary amines are widely recognized within various industrial settings as exceptionally versatile intermediates.<sup>1–4</sup> As a consequence of their value, a number of synthetic methods are available for the production of primary amines.<sup>5,6</sup> Nonetheless, heterogeneously catalyzed hydrogenation of nitriles is commonly employed in an industrial setting.<sup>3,5–7</sup> Conversion of the nitrile functionality is reported to be facile, making this reaction attractive for use in large-scale industrial processes.<sup>4,6,8</sup> Observed alongside the desired hydrogenation pathway, however, are a number of unwanted side reactions.<sup>9,10</sup> Thus, achieving high selectivity toward the primary amine is often challenging. Catalyst selection is recurrently reported to be the determining factor in the product distribution.<sup>1,11</sup> Despite the positive reports for the application of Raney nickel and cobalt catalysts for this reaction,<sup>4</sup> supported palladium catalysts are often employed for more complex reaction systems that possess multiple functionalities.<sup>2,12,13</sup> An example of a palladium-catalyzed nitrile hydrogenation reaction was provided in 2005 by Hegeđús and Máthé,<sup>3</sup> who reported the hydrogenation of benzonitrile to yield benzylamine with high selectivity (95%) under mild conditions (30 °C, 6 bar) over a 10% Pd/C catalyst. This reaction was conducted in a mixture of two immiscible solvents (water and dichloromethane) in the presence of an acid additive ( $NaH_2PO_4$ ). Another example was provided by Beller et al., who also used a 10% Pd/C catalyst for the catalytic transfer hydrogenation of aromatic

nitriles to the corresponding primary amines. In this instance, ammonium formate was employed as a hydrogen donor.<sup>14</sup>

Mechanistic aspects of the single-batch liquid-phase hydrogenation reaction of mandelonitrile (MN) over a carbon-supported palladium catalyst (5 wt % Pd/C) have previously been investigated.<sup>15,16</sup> Alongside the desired product, phenethylamine (PEA), the byproduct 2-amino-1-phenylethanol (2-APE) was produced (Scheme 1). These prior studies indicated that while the reaction was not completely selective toward phenethylamine ( $S = 87\%$ ), a closed mass

**Scheme 1. Liquid-Phase Hydrogenation Reaction of Mandelonitrile (MN) to Afford the Primary Amines 2-Amino-1-phenylethanol (2-APE) and Phenethylamine (PEA)**



Received: March 20, 2020

Published: May 4, 2020



balance was achieved, indicating efficient catalysis under the stated conditions.<sup>15</sup>

In order to evaluate whether catalytic turnover could be sustained over multiple cycles for the specified reaction, a repeat-batch procedure was adopted. Here numerous aliquots of the mandelonitrile starting material and the sulfuric acid auxiliary reagent were made for a single catalyst charge.<sup>15–17</sup> This procedure effectively represents a series of batch reactions. In this case, six sequential additions of the reagents (mandelonitrile and sulfuric acid) were studied. The reaction medium was analyzed off-line by high-performance liquid chromatography (HPLC). With reference to a previously reported reaction scheme,<sup>16</sup> the prospect of sustained catalytic performance was examined in terms of acid concentration, stirrer agitation rate, catalyst mass, and hydrogen availability.

The study highlights the importance of maintaining the hydrogen supply throughout *all* components of this multistage process, which includes both hydrogenation and hydrolysis steps.<sup>16</sup> Furthermore, within this reaction system, reactive imine and enamine intermediates may participate in coupling reactions with the amine products to form the corresponding secondary and tertiary amines,<sup>18–21</sup> thus providing additional routes to those previously described,<sup>15,16</sup> which may compromise product selectivity. Thus, deactivation pathways via oligomer formation are possible.

The formation of oligomeric products by these means was explored by preliminary inelastic neutron scattering (INS) measurements. It is noted, however, that a “technical grade” 5 wt % Pd/C catalyst was used for these measurements, not the commercially available 5 wt % Pd/C catalyst used for the remainder of the study. This difference was due to the requirement of large quantities of spent catalyst, which could not easily be generated at the academic site.

## 2. EXPERIMENTAL SECTION

**2.1. Materials.** Selected as a representative material suitable for use as a generic fine chemicals hydrogenation catalyst, a commercial-grade 5 wt % Pd/C catalyst (Sigma-Aldrich, code no. 205680) was almost exclusively used (sections 3.1–3.6). Characterization of this catalyst is reported elsewhere.<sup>15</sup> Because of the large sample size required for INS ( $\geq 10$  g),<sup>22</sup> a technical-grade 5 wt % Pd/C catalyst was solely used for the INS measurements (Section 3.7). This unspecified technical catalyst is used in the industrial variant of the reaction (hydrogenation of a substituted aromatic cyanohydrin), which is operated as a fed-batch process and exhibits significant catalyst deactivation. Both fresh and spent samples of technical-grade catalyst (extracted from the medium-scale reactor at the industrial site) were examined by INS. Mandelonitrile (Tokyo Chemical Industry, >97% purity) and sulfuric acid (Fisher Scientific, nominally 95–98% H<sub>2</sub>SO<sub>4</sub>) were used as received without further purification. In all instances, methanol (Riedel-de Haën, 99.9% purity) was utilized as the reaction solvent.

**2.2. Hydrogenation Reaction Procedure.** **2.2.1. Single-Batch Operation.** The hydrogenation reactions were carried out in a 500 mL stirred autoclave (Büchi Glas Uster). The reactor was first charged with the catalyst (300 mg) and solvent (310 mL of methanol) prior to being purged with inert gas (nitrogen). The catalyst/solvent mixture was heated and stirred at approximately 300 rpm under 6 barg hydrogen for 1 h in order to reduce the catalyst. Separate measurements using the hydrogenation of benzaldehyde as a test reaction

established that this procedure was sufficient to fully reduce the catalyst. The reaction vessel was heated by silicon oil passed around the reactor via a heating circulator (Julabo, F25). In a separate vessel, the substrate, mandelonitrile (1.46 g, 11 mmol), was combined with 2 molar equiv of sulfuric acid and dissolved in 40 mL of reaction solvent (methanol), and the mixture was degassed under helium.

Once the desired temperature was obtained, the substrate was added, the system was sealed, and the hydrogen charging procedure was commenced. The time taken to reach operational pressure was dependent on the hydrogen gas line manifold pressure, i.e., the back pressure of hydrogen used to charge the reactor via a back-pressure regulator. Two hydrogen line manifold pressures were utilized: 6.5 and 8.0 barg. For an autoclave operational pressure of 6 barg, respective charging times of 7 and 3.5 min were required for the aforementioned hydrogen line manifold pressures. When the designated reaction pressure was attained (typically 6 barg but occasionally 4 barg (section 3.5 only)), agitation was commenced. Reaction time  $t = 0$  was designated as the time when the selected autoclave pressure was attained. As the reaction typically commences during the short hydrogen pressure charging process, hydrogen uptake measurements cannot be reliably monitored during this procedure. However, once the reactor pressure is attained, hydrogen uptake measurements can be used to determine relative hydrogen consumption.

**2.2.2. Repeat-Batch Operation.** Alterations to the single-batch hydrogenation reaction protocol were implemented in order to maximize primary amine production. To this end, a repeat-batch protocol was implemented that was additionally intended to provide information on the repeatability of the phenethylamine synthesis process. Here a procedure identical to that utilized for a single-batch run was initially employed. Then at reaction completion ( $t = 2$  h), the reactor was depressurized, and a second aliquot of degassed reagent (mandelonitrile and acid) without further catalyst was added to the reactor with 10 mL of methanol. Following this, the reactor was recharged with hydrogen until the desired pressure was attained, and the stirring was subsequently recommenced. The reaction was left for a 2 h period as before, prior to sampling. This process was repeated until the desired number of reagent additions (typically six) had been achieved.

Thus, for a single-batch run (section 2.2.1), the catalyst/substrate ratio was rather high at 0.205 (0.300 g/1.46 g). However, this decreased in the repeat-batch runs, and after six aliquots of 1.46 g of mandelonitrile were reacted over 0.3 g of catalyst, the ratio was reduced to value of 0.034 (0.300 g/8.76 g), a value closer to that encountered in representative industrial operations.

**2.3. Determination of Liquid Mass Transfer Coefficients.** Liquid mass transfer coefficients ( $k_{La}$ ) were determined using the dynamic pressure method.<sup>23</sup> The reaction solvent was first degassed with nitrogen to obtain an equilibrium while the temperature of the vessel was increased. Once the desired temperature (40 °C) was reached, the reactor was pressurized to 6 barg with hydrogen. Following this, the motor controlling the agitation speed was switched on at a set value. Immediately after the commencement of agitation, the pressure of the vessel declines as the gas from the headspace of the reactor is adsorbed into the liquid. The pressure of the system continues to decline until a saturation point is reached.<sup>24</sup> By monitoring of the pressure variation as

the adsorption proceeds, the mass transfer coefficient can be calculated using the following equation:<sup>25</sup>

$$\frac{P_f - P_0}{P_i - P_0} \ln\left(\frac{P_i - P_f}{P - P_f}\right) = k_{La}t$$

where  $P_0$  is the solvent vapor pressure,  $P_f$  and  $P_i$  are the final and initial pressures, respectively, and  $P$  is the pressure at a given time  $t$ .  $P_0$ ,  $P_i$ , and  $P$  were obtained experimentally;  $P_0 = 0.35$  bar for methanol at 40 °C.<sup>26</sup> On the basis of this equation, a plot of  $(P_f - P_0/P_i - P_0) \ln(P_i - P_f/P - P_f)$  versus time should then yield a straight line with the gradient defining the mass transfer coefficient, which represents the kinetics of the hydrogen solvation process.

#### 2.4. High-Performance Liquid Chromatography.

Liquid samples were collected periodically and filtered using a 0.22  $\mu\text{m}$  syringe filter (Chromatography Direct, 25 mm, 0.22  $\mu\text{m}$ ) to remove any catalyst residue. All samples, contained in sealed vials, were subsequently quenched in ice prior to analysis by HPLC undertaken using a Hewlett-Packard 1100 series chromatograph fitted with a BDS Hypersil C18 column of dimensions 250 mm  $\times$  4.6 mm. Solvents utilized in gradient mode were analytical-grade water acidified with 1 vol %  $\text{H}_3\text{PO}_4$  and HPLC-grade acetonitrile (Fisher Scientific, 99.9% purity).

All samples were analyzed by UV absorption spectroscopy at a wavelength of 210 nm under a constant flow rate of 1.5 mL  $\text{min}^{-1}$  with the column thermostat fixed at 20 °C. Calibration was carried out on a number of solutions of known concentration, and the standard error was found to be less than  $\pm 5\%$ .

#### 2.5. Inelastic Neutron Scattering.

INS is well-suited to examining heterogeneous catalysts postreaction, as it can provide the vibrational spectrum of black and metallic samples that are otherwise not amenable to investigation by optical methods such as infrared spectroscopy.<sup>22</sup> The INS measurements were performed using the MERLIN spectrometer of the ISIS Facility, which is located at the STFC Rutherford Appleton Laboratory.<sup>27</sup> Two samples of the technical-grade 5 wt % Pd/C catalyst supplied by the industrial partner (Syngenta) were analyzed: (i) a fresh (i.e., unreacted) catalyst and (ii) a postreaction catalyst that was extracted from a fed-batch reactor arrangement employed to hydrogenate an unspecified substituted aromatic cyanohydrin. The latter sample exhibited significant catalyst deactivation characteristics. Prior to spectral acquisition, both samples were dried in a vacuum oven (Thermo Scientific, 3608-6CE) at 80 °C for 12 h. They were then placed within separate aluminum foil sachets and mounted within aluminum INS cells.<sup>28</sup> The INS spectra were recorded at 20 K and at incident energies of 600 and 250 meV. Spectral acquisition at these energies affords access to  $\nu(\text{C-H})$  and  $\delta(\text{C-H})$  vibrational modes while maintaining reasonable resolution in both regions of the spectrum. The "S" chopper package was employed, which afforded maximum sensitivity at these energies.<sup>29</sup> Spectra were analyzed as difference spectra, with the spectrum of the unreacted catalyst sample (i) subtracted from the spectrum of the postreaction sample (ii).

### 3. RESULTS

#### 3.1. From Single Batch to Repeat Batch.

The single-batch liquid-phase hydrogenation reaction of mandelonitrile is reported elsewhere.<sup>15,16</sup> Figure 1 reproduces the reaction profile for optimized performance<sup>15</sup> and shows mandelonitrile

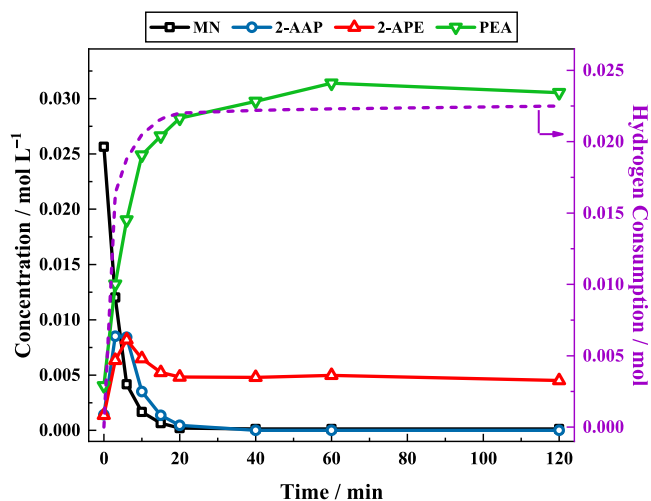


**Figure 1.** Reaction profile and hydrogen uptake curve for a single-batch operation of the hydrogenation reaction of mandelonitrile (11 mmol) with 2 molar equiv of  $\text{H}_2\text{SO}_4$  over 300 mg of 5% Pd/C catalyst. The reaction was carried out at 40 °C, 6 barg hydrogen with an agitation rate of 1050 rpm. [MN = mandelonitrile; 2-AAP = 2-aminoacetophenone; 2-APE = 2-amino-1-phenylethanol; PEA = phenethylamine]. From ref 15. CC BY 3.0.

conversion to be complete within 20 min. Identified as a reaction intermediate, 2-aminoacetophenone (2-AAP) is also consumed within approximately 20 min. Production of both the desired product (phenethylamine) and the byproduct (2-amino-1-phenylethanol) is shown to saturate by approximately  $t = 40$  min.<sup>15,16</sup> At reaction completion, identified by saturation of the hydrogen uptake curve, the selectivities toward phenethylamine and 2-amino-1-phenylethanol are 87% and 13%, respectively.<sup>15,16</sup> Moreover, a complete mass balance indicates the absence of coupling reactions or indeed any other unwanted chemistry.<sup>15</sup> It is noted that the profile for the 2-APE byproduct is somewhat anomalous in passing through a maximum before being maintained at a finite concentration. This profile is found to be reproducible, though its origins are currently unknown.

A generic method of ascertaining the extent to which mass transport controls a catalytic reaction is to run the reaction at several different agitation speeds and monitor the effect on the rate of reagent consumption (Figure 2, blue trace).<sup>30–32</sup> It is shown in Figure 2 that applying an agitation speed of  $\geq 750$  rpm should ensure efficient hydrodynamics for the mandelonitrile hydrogenation system. Operating at agitation speeds lower than this value is likely to lead to a mass transfer limitation at the gas–liquid interface. However, it is noted that the three-phase mandelonitrile hydrogenation system (solid–liquid–gas) constitutes a multistep reaction pathway requiring hydrogen availability throughout the full reaction coordinate.<sup>16</sup> Consequently, the sole analysis of rate of reagent consumption versus agitation speed may not provide the most comprehensive description of hydrogen dissolution for the reaction system as a whole and may result in a misleading outcome.<sup>31–33</sup>

Not considered in the mandelonitrile consumption rate/agitation speed correlation are the subsequent hydrogen-requiring steps necessary to afford phenethylamine. A more rigorous experimental method of ensuring that a process is operating under a maximized hydrogen supply is the determination of the liquid mass transfer coefficient ( $k_{La}$ ).<sup>33</sup>

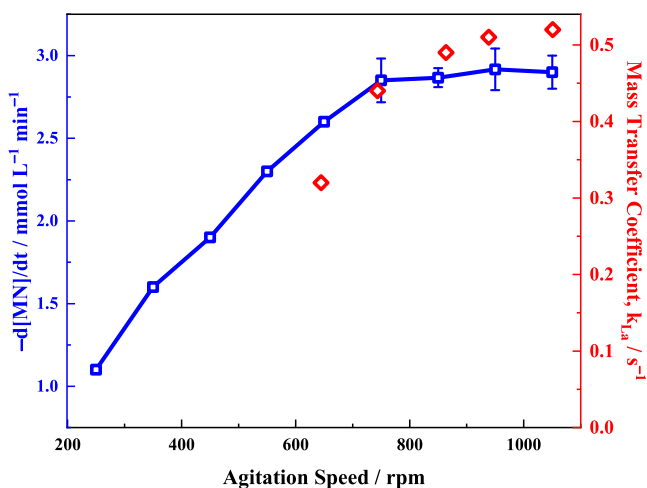


**Figure 2.** Left-hand y axis (blue): Rate of hydrogenation of mandelonitrile (11 mmol in the presence of 2 molar equiv of  $\text{H}_2\text{SO}_4$  under 6 barg hydrogen pressure at 40 °C using 0.3 g of 5% Pd/C catalyst) as a function of reactor stirrer agitation speed. The error bars represent the ranges observed from triplicate measurements. Right-hand y axis (red): Gas–liquid mass transfer coefficient for hydrogen ( $P = 6$  barg) in methanol ( $T = 40$  °C) as a function of reactor stirrer agitation speed.

Figure 2 (red trace) presents  $k_{La}$  as a function of the agitation rate and shows the rate of hydrogen dissolution to be close to a maximum value at the maximum stirring speed (1050 rpm). This outcome is interpreted to indicate that the dihydrogen solvation rate is optimized at elevated agitation rates, with the quantity of dissolved hydrogen in methanol ultimately limited by Henry's law. Thus, to ensure that the reaction vessel operates at its maximum possible efficiency, allowing favorable kinetics for the  $\text{H}_2(\text{g}) \rightarrow \text{H}_2(\text{solv})$  step active at the gas–liquid interface, agitation of the reaction mixture at 1050 rpm is necessary. Finally for this section, it is noted that Figure 2 corresponds to hydrogen demand for the working catalyst. This is a different regime from that of the catalyst reduction that is required to facilitate the less demanding  $\text{Pd}^{2+} \rightarrow \text{Pd}^0$  transition, where lower agitation rates are permissible (section 2.2.1).

**3.2. Optimized Single-Batch Conditions Applied to Repeat-Batch Reactions.** Figure 3 presents six reagent additions over a single charge of catalyst adopting the conditions optimized for a single-batch process (Figure 1) and represents the repeat-batch mode operation of the reactor. By the end of each addition ( $t = 2$  h), complete conversion of the starting material is achieved for all six additions. Production of both phenethylamine and 2-amino-1-phenylethanol is also sustained throughout this sequence. While 2-amino-1-phenylethanol is shown to be produced at a consistent quantity for each addition, closely following the projected rate (dashed lines), phenethylamine formation is seen to drop off for later additions (addition 4 and beyond). The concentration of reagent and products are monitored only at the end of each 2 h addition, and thus, the data cannot be used to obtain rate data for each of the additions. Nonetheless, it is clear from Figure 3 that reduced phenethylamine yields are observed on repeated cycling.

Figure S1 presents the concentration versus time profiles for the first three additions of the six-batch study presented in Figure 3 and shows the mandelonitrile consumption rate to be

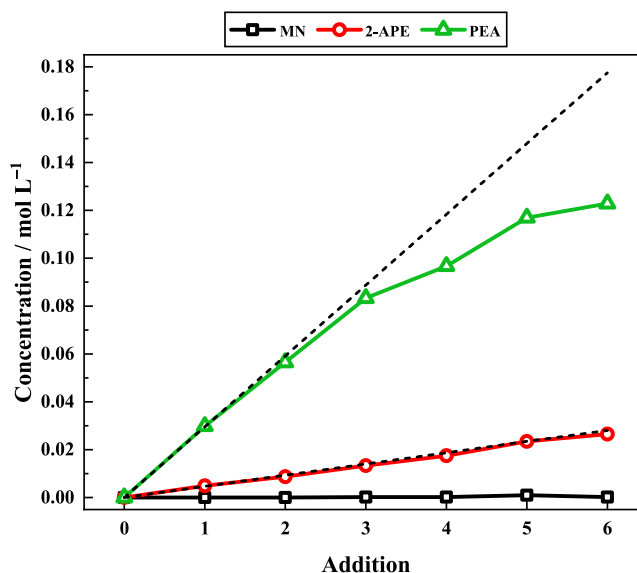
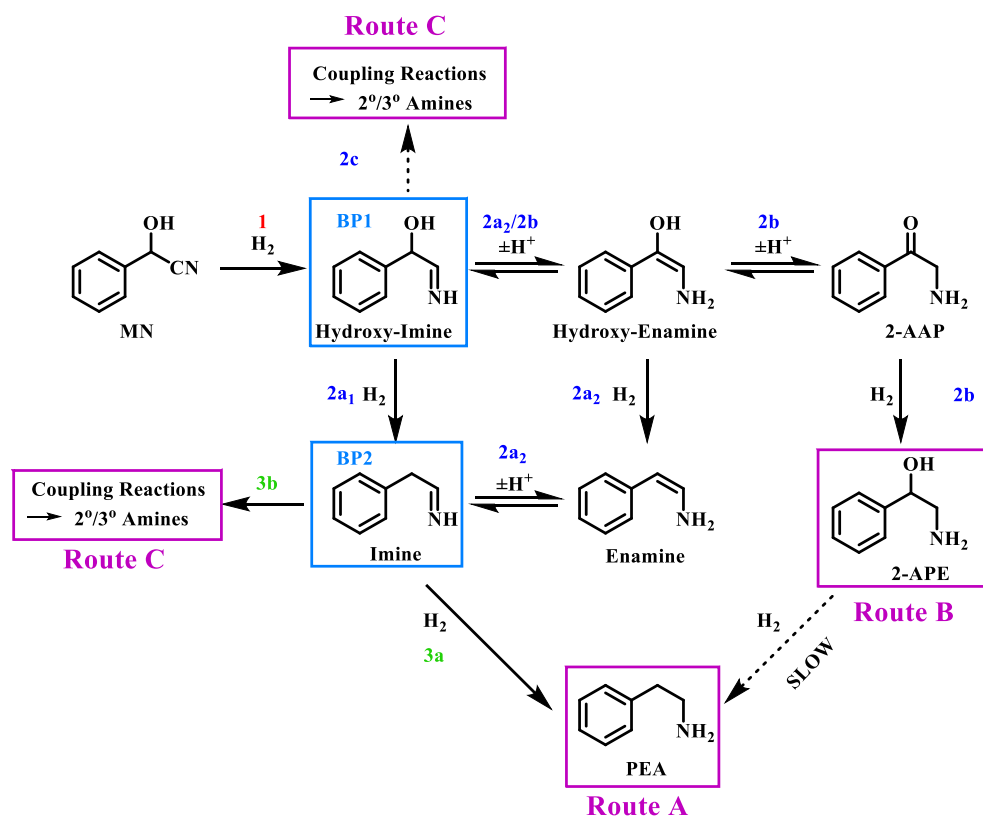


**Figure 3.** Reaction profile for a six-batch mandelonitrile hydrogenation reaction. Each reagent addition comprises mandelonitrile (1.46 g) and 2 molar equiv of  $\text{H}_2\text{SO}_4$ , reacted over the same 5 wt % Pd/C catalyst (300 mg) in methanol. The reaction was conducted at 40 °C under 6 barg hydrogen pressure at an agitation speed of 1050 rpm. Each addition (1–6) represents a fixed 2 h time period. [MN = mandelonitrile; 2-APE = 2-amino-1-phenylethanol; PEA = phenethylamine]. The dashed black lines associated with the 2-amino-1-phenylethanol and phenethylamine data points are representative of predicted continuous product formation based on the product formation rate observed for addition 1.

effectively constant for each run, indicating comparable kinetics for the first three sets of reactions. This is consistent with the catalyst being fully reduced during the initial activation stage (section 2.2.1). Figure S1 also shows reproducible profiles for 2-APE formation, but interestingly, some retardation in the production of the intermediate 2-aminoacetophenone is observed for the third run. With reference to the reaction complexity presented in Scheme 2 (see section 3.3 below), it is thought that the modified 2-AAP profile is an early indicator of an emerging deactivation channel.

Extending the mass balance previously reported for a single-batch run,<sup>16</sup> Figure 4 shows the percentage composition of the reaction mixture at the end of each addition, allowing the selectivity and mass balance to be visualized. Consistently observed for all six additions is the complete consumption of the nitrile. An additional consistency for each of the six additions is the presence of the byproduct 2-amino-1-phenylethanol, which is shown to occupy approximately 14% of the reaction mixture for all additions. In contrast, the desired product (phenethylamine) is shown to occupy between 85% and 87% of the product distribution for additions 1–3, returning a closed mass balance, which indicates that all of the chemistry associated with the first three additions is taken into account. Further examination of the product distribution, however, reveals that the percentage occupied by phenethylamine drops after the third addition resulting in an increasingly incomplete mass balance. By addition 6, the missing mass accounts for approximately 17% of the reaction mixture. Thus, from Figure 4 it is clear that another pathway is accessed later on in the catalyst cycling process (additions 4–6).

Scheme 2. Expansion of the Reaction Scheme for the Hydrogenation Reaction of Mandelonitrile (1.46 g) over a 5% Pd/C Catalyst (300 mg) in Methanol to Include Potential Deactivation Pathways<sup>a</sup>



<sup>a</sup>Three major pathways (routes A–C) are highlighted. The colored numbers are associated with various reaction steps for clarity in later analyses. MN = mandelonitrile; 2-AAP = 2-aminoacetophenone; 2-APE = 2-amino-1-phenylethanol; PEA = phenethylamine. BP1 and BP2 denote branching points 1 and 2, respectively. 1, 2, and 3 represent the hydrogen supply stages required by the reaction. The scheme has been adapted from ref 16. CC BY 4.0.

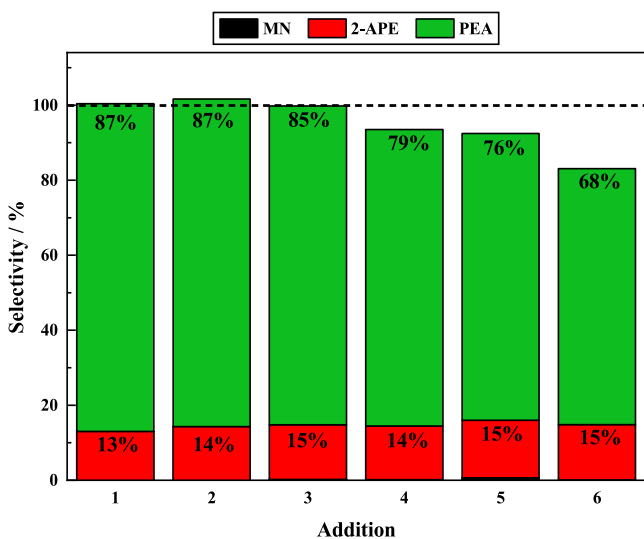


**Figure 4.** Percentage composition of the reaction mixture at the end of each 2 h reaction for a six-batch mandelonitrile hydrogenation reaction. Each reagent addition comprises mandelonitrile (1.46 g) and 2 molar equiv of H<sub>2</sub>SO<sub>4</sub>, reacted over the same 5 wt % Pd/C catalyst (300 mg) in methanol. The reaction was conducted at 40 °C under 6 barg hydrogen pressure at an agitation speed of 1050 rpm. Each addition (1–6) represents a fixed 2 h time period. [MN = mandelonitrile; 2-APE = 2-amino-1-phenylethanol; PEA = phenethylamine].

This deviation from a closed mass balance coincides with a number of extra features in the chromatograms observed at higher retention times, a scenario consistent with the formation of secondary and tertiary amines. In the case of 4-hydroxybenzyl cyanide hydrogenation over Pd/C, secondary and tertiary amine formation could be identified and quantified because of the relative simplicity of that particular reaction system.<sup>17</sup> In this instance, however, such identification and quantification was not possible because of the complexity and multiplicity of the coupling products formed. It is proposed that the mass imbalance observed in Figure 4 is due to oligomeric product both in the liquid phase and bound to the surface of the catalyst in an unspecified ratio.

**3.3. Experimental Findings Are Linked to the Reaction Scheme.** Previous mechanistic studies conducted on the mandelonitrile hydrogenation system have culminated in the proposal of a complex, multistep reaction scheme that has been validated against the outcome of a single-batch hydrogenation reaction.<sup>15,16</sup> In combination, Figures 3 and 4 illustrate that repeat cycling of the catalyst reveals additional chemistry that is unobservable under single-batch conditions (Figure 1). Scheme 2 therefore presents an expanded reaction scheme that accounts for the occurrence of coupling pathways leading to secondary and tertiary amine formation as well as possible surface-bound oligomer entities. Irreversible binding of the latter species to the catalyst surface via the amine

functionality could contribute to deactivation of the catalyst due to reduced availability of active sites.<sup>19–21</sup>

Up to this point, analysis has primarily focused on phenethylamine production. However, Scheme 2 highlights that additional routes that do not culminate in phenethylamine are available within the mandelonitrile hydrogenation system. Accordingly, routes A–C are highlighted in Scheme 2; each route possesses a different hydrogen requirement and a unique outcome. In the first instance, the routes commence with a common transformation; namely, hydrogenation of the nitrile moiety of mandelonitrile to form the hydroxyimine intermediate (stage 1). Thereafter, Scheme 2 shows that the reaction may take one or more of three major routes. Consequently, the hydroxyimine represents a branching point and thus is denoted as BP1 in Scheme 2.

Following hydroxyimine formation, route A affords the desired primary amine product, phenethylamine, in a stepwise process requiring 3 molar equiv of dihydrogen. With reference to Scheme 2, it is observed that at BP1, route A follows path 2a<sub>1</sub> to form the imine. It is here that the second branching point in the reaction (BP2) is reached. The concluding step for route A is the occurrence of path 3a to yield phenethylamine. Furthermore, for completeness, it should be noted that at BP1 the hydroxyimine can undergo tautomerization to the hydroxyenamine by following path 2a<sub>2</sub>. Hydrogenolysis of the hydroxyenamine to furnish the enamine followed by a second reverse acid-catalyzed tautomerization reaction to give the imine then precedes the final step, 3a, to give phenethylamine. In addition, to rationalize the reported order of events, it has been evidenced in previous kinetic<sup>15</sup> and deuteration<sup>16</sup> studies that hydrogenation of the enamine to phenethylamine is not possible under the presented reaction conditions.

Conversely, if the reaction is to follow route B, then at BP1 path 2b is taken. It is noted that the tautomerization from the hydroxyimine to the hydroxyenamine is labeled as both 2a<sub>2</sub> and 2b. This transformation is common to routes A and B and has hence been labeled according to both routes to avoid ambiguity. Once path 2b has been taken to the hydroxyenamine, keto–enol tautomerization to afford the detectable intermediate 2-aminoacetophenone occurs. These tautomeric pathways occur prior to the second hydrogenation step. Hydrogenation of 2-aminoacetophenone rapidly affords the byproduct 2-amino-1-phenylethanol, the hydrogenolysis of which has been shown previously to be kinetically hindered.<sup>15</sup> It is acknowledged that it is also feasible for the hydroxyimine and the hydroxyenamine to undergo direct hydrogenolysis to 2-amino-1-phenylethanol. Nonetheless, an unpublished outcome from the previous deuteration study suggests that these reactions do not occur.<sup>16</sup> To definitively establish this deduction, further work is required. For the purpose of clarity, these transformations have been excluded from Scheme 2. Consequently, it is identified that route B requires 2 molar equiv of dihydrogen to afford 2-amino-1-phenylethanol.

Finally, route C proceeds from either BP1 or BP2. Instead of incurring a hydrogenation or hydrogenolysis step, the hydroxyimine and/or imine intermediates participate in coupling reactions to form secondary or tertiary amines alongside unwanted oligomeric products. The production of these higher amine species is recurrently reported to reduce the selectivity toward the desired product.<sup>18–20</sup> Route C requires either 1 or 2 molar equiv of dihydrogen. The quantity of dihydrogen required is dependent on whether route C proceeds from BP1 or BP2 and corresponds to formation of

the hydroxyimine (BP1 and BP2) and subsequent hydrogenolysis of the hydroxyimine (BP2).

In order to establish which routes are operational at a given point in the catalytic cycle, an outcome specific to each specified route (A–C) must be identified. For route A, Scheme 2 shows that phenethylamine is the expected product, and therefore, if route A remains operational, continuous production of phenethylamine will be observed. If route B is active, however, it will involve a buildup of 2-amino-1-phenylethanol. Finally, if route C is occurs, it is likely that there will be formation of a carbonaceous overlayer on the catalyst surface due to the production of the oligomeric products associated with coupling reactions. This outcome will manifest itself as missing mass, as the above-mentioned oligomeric products are expected to be retained at the catalyst surface.<sup>34</sup> Consequently, the route or routes that the reaction takes will dictate the product outcome. Analysis of the product distribution can thus be used as a diagnostic tool to monitor the activity of the catalyst as it is cycled, which is an enticing and potentially revealing prospect.

For the single-batch mandelonitrile hydrogenation reaction (Figure 1), both routes A and B are seen to be operational, with route A dominating. Route C is inoperative, as evidenced by the complete mass balance.<sup>15</sup> It is acknowledged that route C may be operative but undetectable under these conditions. It is possible that despite the positive outcome of Figure 1, oligomeric product may have begun to bind to the catalyst surface, but crucially, there was sufficient active catalyst to allow the reaction to reach completion. Therefore, if catalyst activity is sustained upon cycling, it is to be expected that as each substrate addition is made, production of both phenethylamine and 2-amino-1-phenylethanol will be observed. Notably, the selectivity of the product mixture should remain unaltered. Indeed, Figures 3 and 4 show that routes A and B are sustained effectively for additions 1–3 without any major selectivity changes, as would be predicted if the catalyst activity were fully maintained. However, upon further monitoring (additions 4–6) it is seen that in addition to the decline of route A, route C is invoked, as demonstrated by the missing mass observed for later additions (Figure 4).

Expanding these molecular considerations, Scheme 2 defines the hydrogen requirement for each route, allowing further predictions regarding the resultant product distribution under altered experimental conditions to be made. It is hence proposed that the product distribution can be used as a diagnostic tool to ascertain the hydrogen availability in the system at a given time in the cycling process. Route A dominates the surface hydrogen requirement and thereby sets a threshold concentration of  $H_{ads}$  throughout the full reaction coordinate that is necessary to support sustained turnover. Maintenance of that threshold concentration enables the reaction to proceed as indicated in Figure 1. However, should  $[H_{ads}]$  fall below this threshold value, the hydrogen can be partitioned elsewhere, thereby modifying the reaction profile. In this way, the product distribution becomes an indicator of hydrogen supply at the Pd surface. Specifically, under hydrogen-lean conditions homogeneous processes may be favored over heterogeneous processes. Thus, routes that require a lower number of heterogeneous processes will be enhanced compared with their single-batch output.

Adding further complexity, it is additionally surmised that surface hydrogen also has a role in maintaining the active Pd sites and mitigating against possible carbon deposition

processes (via dissociative adsorption of reagent/intermediates/products). Hence, diminution of route A due to constrained availability of  $H_{ads}$  not only can facilitate hydrogen partitioning into routes B and C but also can induce a reduction in the number of available active sites and thus constitutes a catalyst deactivation channel.

**3.4. Role of the Acid Additive.** Included in the reaction mixture for the optimized reaction conditions (Figure 3) is a sulfuric acid additive. Investigation of this substrate system has highlighted that the presence of this additive is essential for the conversion of mandelonitrile to be achieved.<sup>15</sup> The primary role of the acid is to protonate the amine functionality of the products, thus preventing these species from acting as nucleophiles and participating in coupling reactions with the imine intermediates (paths 2c and 3b to afford route C products; Scheme 2). Moreover, the resultant salt is kept in the liquid phase and hence is prohibited from strongly chemisorbing to the palladium surface via the nitrogen lone pair and acting as a catalyst poison.<sup>35–37</sup>

Further to its essential amine protonation function, the acid present in the reaction mixture also has a catalytic role in that it is responsible for the formation of the intermediate 2-aminoacetophenone via a tautomeric pathway originating at the hydroxyimine.<sup>15</sup> The standard reaction conditions include 2 molar equiv of sulfuric acid with respect to the starting nitrile concentration (section 2.1). Because  $H_2SO_4$  is a diprotic acid, Figure 1 shows that the quantity used for the reaction exceeds the requirement for protonation purposes. However, as the acid additive has an established role in the aforementioned homogeneous chemistry, it is necessary to speculate that the acid may also catalyze additional homogeneous reactions within the system. It can then be postulated that additional acid-catalyzed side reactions could provide a further source for the missing mass observed for later additions under the optimized reaction conditions (Figure 4).

To enable elucidation of any potential issues associated with the presence of excess quantities of a strong acid in the reaction mixture, a reduced quantity of acid (1 molar equiv with respect to the nitrile) was added with each aliquot of starting material; the results of this are presented in Figure 5 and compared with the reference profile (Figure 3). Figure 5 quite vividly highlights that lowering the concentration of acid in the system results in detrimental alterations to the six-batch reaction profile. In stark contrast to the optimized conditions (dashed lines, Figure 5), full nitrile conversion under the acid-poor conditions is achieved for one addition only. From addition 2 onward, there is incomplete conversion of the starting material, resulting in buildup of this species in the reaction mixture. Moreover, production of both the byproduct and the desired product is shown to be significantly hindered under these conditions. Route A is stunted from the outset, with phenethylamine production shown to be only 23% of that under the optimized reaction conditions (Figure 3). Indeed, no further production of phenethylamine was detected throughout the course of the reaction, indicating the preferential deactivation of route A under acid poor conditions. Route B, however, is shown to be slightly more robust, with the formation of 2-amino-1-phenylethanol sustained for two additions before a product formation plateau is reached. Over the six addition processes, both route A and route B experience deactivation. It is proposed that route C is significantly enhanced as a direct consequence of this. Indeed, missing mass is detected from the onset of the reaction,

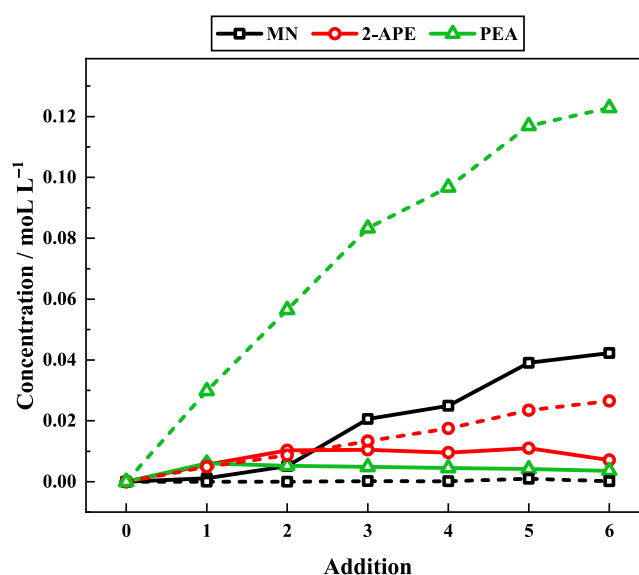


**Figure 5.** Reaction profile for a six-batch mandelonitrile hydrogenation reaction. Each reagent addition comprises mandelonitrile (1.46 g) and either 1 molar equiv (solid lines) or 2 molar equiv (dashed lines) of  $H_2SO_4$ , reacted over the same 5 wt % Pd/C catalyst (300 mg) in methanol. The reaction was conducted at 40 °C under 6 barg hydrogen pressure at an agitation speed of 1050 rpm. Each addition (1–6) represents a fixed 2 h time period. [MN = mandelonitrile; 2-APE = 2-amino-1-phenylethanol; PEA = phenethylamine].

occupying 58% of the reaction mixture at addition 1. The missing mass detected then gradually increases until by addition 6 71% of the mass in the system is unaccounted for.

The altered product distribution under the acid-poor conditions (Figure 5) can be rationalized in terms of the reduced acid presence being insufficient to protonate the entirety of the amine product, leaving these species vulnerable to coupling reactions (route C). Moreover, the occurrence of route C progressively hinders the desired function of the catalyst through blockage of the active sites. Both routes A and B are consequently affected by this. Route A, however, is shown to deactivate earlier in the cycling process than route B. It is postulated that because route A has a greater number of hydrogen-requiring steps to reach its designated product than route B (Scheme 2), route A preferentially deactivates. These experiments therefore establish that a minimum acid concentration is required for continuous conversion of mandelonitrile to afford phenethylamine.

**3.5. Role of the Hydrogen Supply.** The complex nature of the mandelonitrile hydrogenation reaction (Scheme 2) means that there is a significant total hydrogen requirement to afford the desired product. Consequently, once the aforementioned acid requirement (section 3.4) has been satiated, it is essential that the hydrogen supply to the reaction mixture be considered.

The effects of the hydrogen supply can be visualized in Figure 6, where the optimized reaction conditions (dashed lines) are compared to a repeat-addition reaction with extended hydrogen recharging times. In the latter instance, the external manifold line pressure was lowered to 6.5 barg, which had the consequence of increasing the hydrogen recharging time. This parameter relates specifically to the employment of the repeat-batch mode. In this mode, the autoclave hydrogen overpressure is periodically reduced in

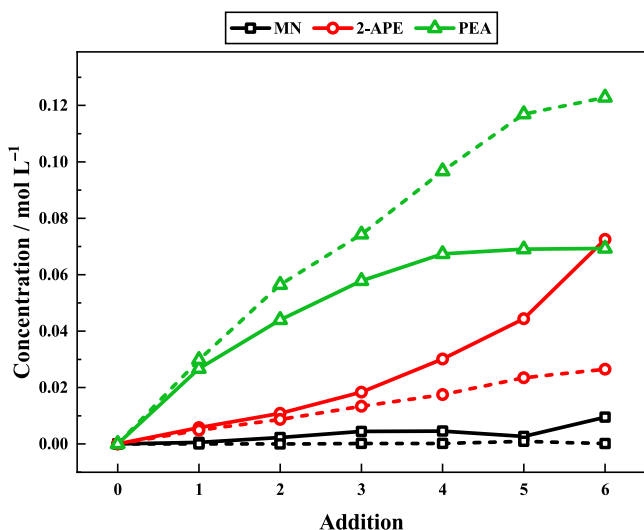


**Figure 6.** Reaction profile for a six-batch mandelonitrile hydrogenation reaction. Each reagent addition comprises mandelonitrile (1.46 g) and 2 molar equiv of  $\text{H}_2\text{SO}_4$ , reacted over the same 5 wt % Pd/C catalyst (300 mg) in methanol. The reaction was conducted at 40 °C under 6 barg hydrogen pressure at an agitation speed of 1050 rpm. The dashed lines represent a manifold line pressure of 8 barg, corresponding to a charging time of 3 min, while the solid lines represent a gas manifold line pressure of 6.5 bar, with an associated charging time of 7.5 min. Each addition (1–6) represents a fixed 2 h time period. [MN = mandelonitrile; 2-APE = 2-amino-1-phenylethanol; PEA = phenethylamine].

order to facilitate the repeat addition of the starting material (plus the acid auxiliary). As a consequence of this operational mode, the external manifold line pressure has an influential role on the time required to recharge the reactor with hydrogen to the desired pressure. During the charging protocol, the reactor experiences short periods associated with limited availability of hydrogen due to the reduced pressure and agitation. With reference to section 3.3, which introduced a dual role for adsorbed hydrogen, namely, reagent conversion and maintenance of Pd active sites, it is thought that the latter role is diminished under conditions of low solvated dihydrogen concentration. Thus, accessible metal surface area is decreased. This leads to a reduced supply of adsorbed hydrogen atoms (formed via the dissociative adsorption of  $\text{H}_2(\text{solv})$ ); such a scenario constrains route A and provides the opportunity for the homogeneous processes associated with route B to proliferate. Furthermore, route C is also thought to experience a degree of enhancement under hydrogen-lean conditions. It is thus proposed that the reduction of hydrogen overpressure in the autoclave has negative consequences in terms of possible fouling of the catalyst during the necessary charging periods.

Whereas the two sets of reaction conditions shown in Figure 6 employ the same agitation rate and hydrogen pressure, Figure S2 further explores the matter of hydrogen supply by keeping the hydrogen recharging time constant at 3 min (manifold line pressure = 8 barg) but explicitly considers the situation of a lower hydrogen operating pressure (4 barg) and agitation rate (600 rpm). Interestingly, Figure S2 shows the deviation from ideal operating conditions to be less dramatic than that presented in Figure 6, indicating the hydrogen recharging time to be a principal parameter affecting sustained product yields during operation in repeat-batch mode.

Collectively, these results indicate that there is an additional requirement to develop experimental protocols that avoid periods where the hydrogen overpressure is periodically cycled. It is thought that (i) fed-batch (semibatch) operation or (ii) utilization of a continuous stirred tank reactor may facilitate this requirement. Unfortunately, neither of these two modes was readily accessible in the facility used for this study.

**3.6. Hydrogen Supply and Diffusional Constraints: A Balance.** It was deduced in section 3.1 that the reactor was operating at its maximum possible efficiency for the provision of hydrogen at the gas–liquid interface. As agitation has a more profound effect on gas–liquid transport than liquid–solid transport,<sup>32</sup> the catalyst mass dependence can be utilized to evaluate liquid–solid limitations within the reaction system.<sup>32</sup>

Figure 7 shows the effect of the catalyst mass on the rate of phenethylamine formation for a single-batch process and

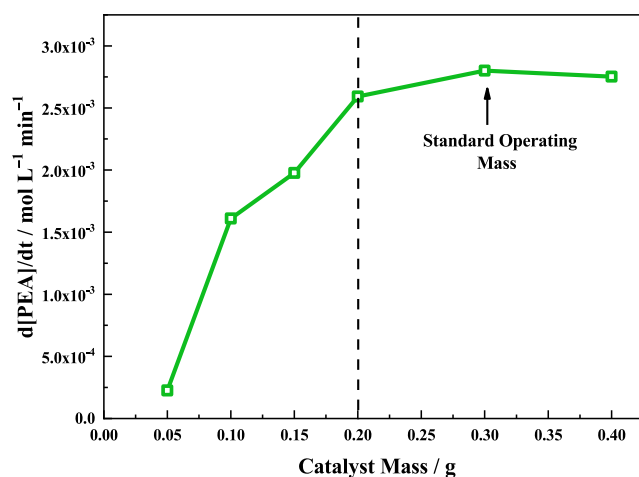


**Figure 7.** Effect of catalyst mass on the rate of formation of phenethylamine for the single-batch hydrogenation reaction of mandelonitrile (1.46 g) over a 5% Pd/C catalyst in the presence of 2 molar equiv of  $\text{H}_2\text{SO}_4$  at 1050 rpm with a hydrogen pressure of 6 barg at 40 °C. The dashed vertical line provides an indication of where the graph reaches a plateau.

indicates that the product formation rate increases linearly with increasing catalyst mass until a saturation point is reached where further increases in the catalyst mass no longer enhance the rate. The standard operational catalyst mass of 300 mg (section 2.2.1) appears on the plateau region of the graph, as indicated in Figure 7. The origin of the plateau region is attributed to mass transport limitations. At low catalyst masses, the rate of phenethylamine production is directly proportional to the catalyst mass, indicating that the production of adsorbed hydrogen atoms ( $\text{H}(\text{ads})$ , formed via the dissociative adsorption of  $\text{H}_2(\text{solv})$  at the Pd crystallites) is unimpeded by the availability of solvated dihydrogen,  $\text{H}_2(\text{solv})$ . Increasing the catalyst mass above approximately 200 mg nudges the  $\text{H}(\text{ads})$  formation rate above the dihydrogen solvation rate, leading to saturation of product formation.

One possibility to alleviate these mass transport limitations at the solution–solid interface is to examine a six-batch hydrogenation reaction sequence using a reduced catalyst mass (100 mg); the results are presented in Figure 8. The two profiles shown in Figure 8 (catalyst mass = 300 mg compared with catalyst mass = 100 mg) show vastly different outcomes. From the reduced catalyst mass profile (100 mg sample; Figure



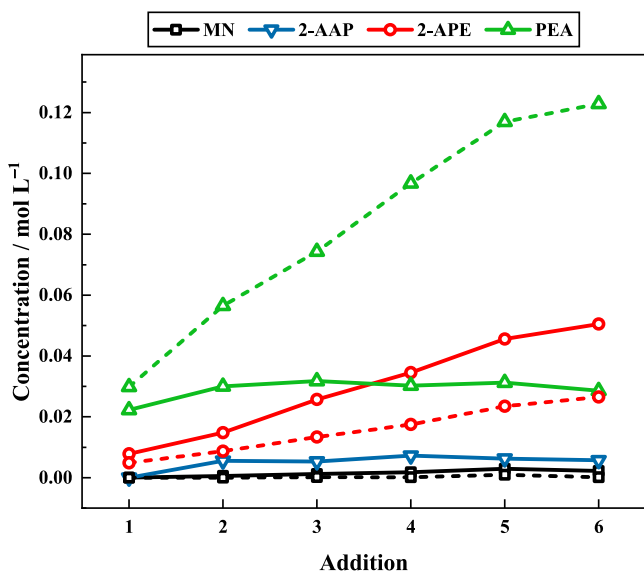


**Figure 8.** Reaction profile for a six-batch mandelonitrile hydrogenation reaction. Each reagent addition comprises mandelonitrile (1.46 g) and 2 molar equiv of  $\text{H}_2\text{SO}_4$ , reacted over the same 5 wt % Pd/C catalyst in methanol. The dashed lines represent the optimized catalyst mass (300 mg) while the solid lines represent a reduced catalyst mass (100 mg). The reaction was conducted at 40 °C under 6 barg hydrogen pressure at an agitation speed of 1050 rpm. Each addition (1–6) represents a fixed 2 h time period. [MN = mandelonitrile; 2-AAP = 2-aminoacetophenone; 2-APE = 2-amino-1-phenylethanol; PEA = phenethylamine].

8 solid lines) it is observed that from addition 2 onward, there is no further production of phenethylamine, indicating that route A has been obstructed by the reduced quantity of catalyst. The production of 2-amino-1-phenylethanol, however, is enhanced, highlighting that route B is favored when the catalyst mass is lowered; in section 3.5 this attribute was associated with a reduced hydrogen supply. Additionally observed is a buildup of the intermediate species 2-aminoacetophenone, an entity not observed for the 300 mg sample (Figure 8, dashed lines). Previous work from this group has shown the conversion of 2-aminoacetophenone to 2-amino-1-phenylethanol to be kinetically fast.<sup>15</sup> Scheme 2 shows that the hydrogenation of 2-aminoacetophenone is the second hydrogen-requiring step in the production of 2-amino-1-phenylethanol (route B). The detection of 2-aminoacetophenone from addition 2 onward implies that this facile reaction has become kinetically hindered, presumably because of a restricted supply of H(ads) as a result of the reduced Pd surface area.

The matter of hydrogen supply at the catalyst surface and product selectivity can be further rationalized with reference to Scheme 2, which indicates that in order to successfully obtain phenethylamine, two branching points must be passed, each requiring an unhindered supply of adsorbed hydrogen atoms. When the mass of catalyst is reduced, however, there are fewer active sites to which hydrogen can adsorb, thus reducing the surface hydrogen availability. When H(ads) is limited, the homogeneous routes (B and C) will be favored over the heterogeneous route (A) at each of the branching points. Thus, the predominance of routes B and C, manifested as enhanced 2-amino-1-phenylethanol and missing mass, respectively (53% missing mass detected by addition 6), and the deactivation of route A can be effectively rationalized.

If a range of catalyst masses are considered, it becomes clear that the mass of catalyst used is critical in maximizing the selectivity toward phenethylamine. Figure 9 illustrates the

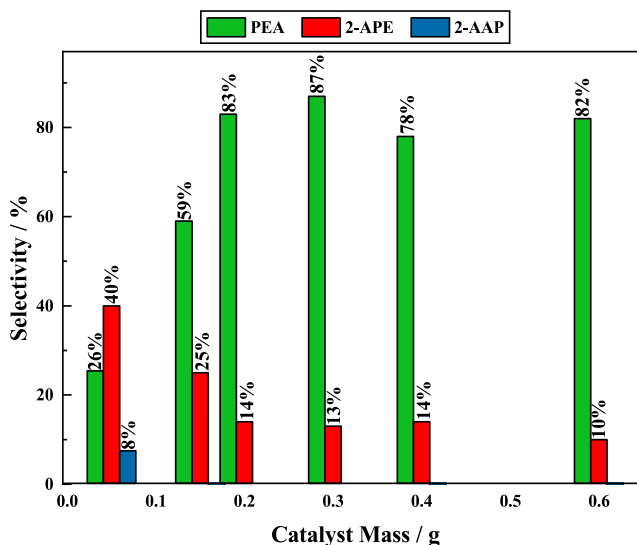


**Figure 9.** Effect of the catalyst mass on the selectivity for a single-batch run for the hydrogenation reaction of mandelonitrile (1.46 g) over a 5 wt % Pd/C catalyst in the presence of 2 molar equiv of  $\text{H}_2\text{SO}_4$  at 1050 rpm with a hydrogen pressure of 6 barg at 40 °C. [PEA = phenethylamine; 2-APE = 2-amino-1-phenylethanol; 2-AAP = 2-aminoacetophenone].

effect of the catalyst mass on the selectivity at reaction completion for a single-batch reaction. The selectivity toward the 2-amino-1-phenylethanol byproduct is shown here to decrease as the catalyst mass is increased, until a critical mass is reached where this selectivity plateaus. The selectivity toward the desired product, however, appears to increase, reaching an approximate plateau at about 200 mg of catalyst.

Figure 9 is interpreted to indicate that a mass of catalyst within the range 200–300 mg represents a position where the rate of product formation is roughly in balance with the provision of surface hydrogen, H(ads). Lower catalyst masses (<200 mg) can be linked to a regime of insufficient H(ads), whereas at higher catalyst masses (>300 mg) the reaction is impeded because of a limited solubilization rate of  $\text{H}_2(\text{g})$ , as suggested by Figure 7. Thus, for sustained production of phenethylamine, the correct balance needs to be sought in terms of efficient replenishment of solvated dihydrogen (>750 rpm agitation rate) within the Henry's law solubilization limit and production of H(ads) at a rate that is greater than the kinetic requirement of the mandelonitrile  $\rightarrow$  phenethylamine transformation rate.

Against this heightened awareness of parameters contributing to sustained phenethylamine yield, it is informative to re-examine Figures 3 and 4 to surmise why the product formation rate is retarded from the fourth addition onward. One possibility is that despite relatively favorable conditions, a small but undetectable amount of oligomer formation occurs during the course of additions 1–3. This formation is progressive until it becomes indirectly observable in the form of a mass imbalance from addition 4 onward. As considered above, oligomerization reduces the active surface area, which reduces the availability of chemisorbed hydrogen atoms for reaction, leading to decreased product yields.

**3.7. Inelastic Neutron Scattering of a Spent (Deactivated) Technical-Grade Catalyst.** The production of higher amines and oligomeric products have thus far been mentioned only in passing. The chromatographic output from the mandelonitrile hydrogenation reaction reveals the presence of a number of unidentified species at high retention times. Because of the complex nature of this reaction system, identification of these species was not possible. In a similar study on the relatively simpler hydrogenation of 4-hydroxybenzyl cyanide, the corresponding secondary and tertiary amines were identified and quantified by  $^1\text{H}$  NMR spectroscopy.<sup>17</sup> As well as being present in the liquid phase, the oligomeric products may be retained at the catalyst surface. Therefore, both the unidentified chromatographic species and the surface-bound species are not identified by the HPLC analysis of the reaction medium. The presence of route C has hence been indirectly implied by inspection of the reaction mass balance (section 3.3). Against this background, the use of inelastic neutron scattering to probe the technical catalyst postreaction for evidence of the formation of a hydrocarbonaceous overlayer is employed in order to overcome this detection difficulty. INS is a useful technique for obtaining the vibrational spectrum of spent technical-grade catalysts, as such materials typically present a significant challenge for conventional optical probes such as infrared spectroscopy.<sup>38</sup> Figure 10 presents the INS difference spectrum of a

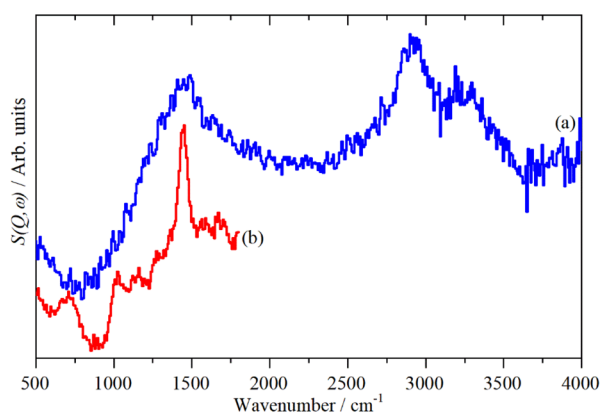


**Figure 10.** INS difference spectra of a spent 5 wt % Pd/C technical-grade catalyst applied to cyanohydrin hydrogenation (deactivated catalyst exhibiting minimal hydrogenation activity after experiencing continuous operation in an industrial fed-batch reactor). The difference spectrum corresponds to the subtraction of the spectrum of an unused sample from that of the postreaction sample. Thus, the difference spectrum corresponds to the spectrum of material retained at the catalyst surface. The spectral range 500–4000  $\text{cm}^{-1}$  (a) was recorded with an incident energy of 600 meV, while an incident energy of 250 meV was utilized for the spectral range 500–1800  $\text{cm}^{-1}$  (b).

deactivated 5 wt % Pd/C technical-grade catalyst that was used in the hydrogenation of aromatic cyanohydrins operated in a medium-scale fed-batch configuration operated by the industrial sponsor (Syngenta).

Figure 10 is characterized by peaks at 3250, 2915, 1660, 1575, 1440(s), 1270, 1160, 1025, and 710  $\text{cm}^{-1}$ . The peaks at 3250 and 2915  $\text{cm}^{-1}$  are respectively assigned to the N–H stretch of an aliphatic secondary amine and the unresolved symmetric and asymmetric C–H stretch modes of  $\text{CH}_2$  groups. The strong peak at 1440  $\text{cm}^{-1}$  is assigned as the

$\text{CH}_2$  scissor mode, with the associated twist and rock modes at 1270 and 710  $\text{cm}^{-1}$ . The weak bands at 1660, 1575, and 1020  $\text{cm}^{-1}$  are assigned as aromatic C–C stretch and C–H bend modes.<sup>39</sup> The corresponding aromatic C–H stretch modes (expected around 3000–3100  $\text{cm}^{-1}$ ) are hidden by the more intense aliphatic and amine stretch modes. Since spectral intensity in INS is directly related to the number of hydrogenaceous entities present in the neutron beam,<sup>40</sup> the low intensity of the bands observed in Figure 10 indicates that only small quantities of hydrocarbonaceous residues are present at the catalyst surface. Collectively, these features are consistent with formation of a hydrocarbonaceous overlayer at the catalyst surface. Specifically, it is attributed to an oligomeric overlayer that is believed to have been formed via either the hydroxyimine species following path 2c at BP1 or the imine species via path 3b at BP2, as identified in Scheme 2. The retained material blocks active sites and is linked to the deactivation of the technical-grade catalyst. The presence of an oligomeric overlayer is consistent with the presence of route C as presented in Scheme 2.

It is noted that carbon-supported metal catalysts are notoriously difficult to characterize but, nevertheless, INS as applied here is able to access the vibrational spectrum of a postreaction heterogeneous catalyst sample. As outlined in section 2.1, the laboratory study outlined in sections 3.1–3.6 is a mimic of a medium-scale industrial process that was not able to provide sufficient quantities of spent catalyst (technical-grade catalyst, 10–20 g) required for the INS measurement. Given the modest mass of catalyst utilized in the laboratory studies (0.3 g), it was not practical to acquire INS spectra with a respectable signal-to-noise ratio for those samples.

#### 4. CONCLUSIONS

The development of the single-batch liquid-phase hydrogenation of mandelonitrile over a 5 wt % Pd/C catalyst has been investigated such that production of the desired primary amine product (phenethylamine) can be optimized. To achieve this, repeat-batch technology, which aims to replicate fed-batch methodology, was employed with a series of six substrate additions over the same catalyst being monitored. The following deductions are made:

- The previously reported reaction scheme for the hydrogenation of mandelonitrile has been expanded to include potential deactivation pathways, which become observable upon catalyst cycling.
- Three pathways have been assigned (routes A–C), each yielding a unique product, which allows the product distribution to be used as a mechanistic diagnostic tool.
- Sustained phenethylamine production requires a minimum acid concentration alongside maintenance of hydrogen availability at the gas–liquid and liquid–solid interfaces. The catalyst mass dictates the availability of chemisorbed hydrogen atoms within the limitations of hydrogen solubility in the process solvent.
- Within the limitations of the present setup, phenethylamine is continuously produced for six substrate additions, with deactivation observed only after addition 4.
- The inelastic neutron scattering spectrum of a spent technical-grade 5 wt % Pd/C catalyst utilized in an industrial-scale fed-batch hydrogenation of a substituted aromatic cyanohydrin indicates the presence of oligo-

meric amine moieties, which are thought to be responsible for attenuation of the catalytic performance.

## ■ ASSOCIATED CONTENT

### Supporting Information

The Supporting Information is available free of charge at <https://pubs.acs.org/doi/10.1021/acs.oprd.0c00111>.

Reaction profiles for the initial three additions of a six-batch mandelonitrile hydrogenation reaction (Figure S1) and reaction profiles for six-batch runs of the hydrogenation reaction of mandelonitrile under “hydrogen-lean” and “hydrogen-rich” conditions (Figure S2) (PDF)

## ■ AUTHOR INFORMATION

### Corresponding Author

David Lennon – School of Chemistry, University of Glasgow, Glasgow G12 8QQ, U.K.; [orcid.org/0000-0001-8397-0528](https://orcid.org/0000-0001-8397-0528); Phone: +44-141-330-4372; Email: [David.Lennon@glasgow.ac.uk](mailto:David.Lennon@glasgow.ac.uk)

### Authors

Mairi I. McAllister – School of Chemistry, University of Glasgow, Glasgow G12 8QQ, U.K.

Cédric Boulho – School of Chemistry, University of Glasgow, Glasgow G12 8QQ, U.K.

Colin Brennan – Syngenta, Jealott's Hill International Research Centre, Bracknell, Berkshire RG42 6EY, U.K.

Stewart F. Parker – ISIS Facility, STFC Rutherford Appleton Laboratory, Chilton, Oxon OX11 0QX, U.K.; [orcid.org/0000-0002-3228-2570](https://orcid.org/0000-0002-3228-2570)

Complete contact information is available at <https://pubs.acs.org/doi/10.1021/acs.oprd.0c00111>

### Notes

The authors declare no competing financial interest.

## ■ ACKNOWLEDGMENTS

Syngenta, the University of Glasgow, and the EPSRC (Grant EP/M508056/1) are thanked for the award of a Ph.D. studentship (M.I.M) and project support. STFC is thanked for the provision of neutron beamtime.

## ■ REFERENCES

- (1) Bagal, D. B.; Bhanage, B. M. Recent Advances in Transition Metal-Catalyzed Hydrogenation of Nitriles. *Adv. Synth. Catal.* **2015**, *357* (5), 883–900.
- (2) Bakker, J. J. W.; van der Neut, A. G.; Kreutzer, M. T.; Moulijn, J. A.; Kapteijn, F. Catalyst performance changes induced by palladium phase transformation in the hydrogenation of the hydrogenation of benzonitrile. *J. Catal.* **2010**, *274*, 176–191.
- (3) Hegedűs, L.; Máthé, T. Selective heterogeneous catalytic hydrogenation of nitriles to primary amines in liquid phase: Part I: Hydrogenation of benzonitrile over palladium. *Appl. Catal., A* **2005**, *296*, 209–215.
- (4) Bawane, S. P.; Sawant, S. B. Reaction kinetics of the liquid-phase hydrogenation of benzonitrile to benzylamine using Raney nickel catalyst. *Chem. Eng. J.* **2004**, *103*, 13–29.
- (5) Miriyala, B.; Bhattacharyya, S.; Williamson, J. S. *Tetrahedron* **2004**, *60*, 1463–1471.
- (6) Neumann, J.; Bornschein, C.; Jiao, H.; Junge, K.; Beller, M. Hydrogenation of aromatic nitriles using a defined ruthenium PNP pincer catalyst. *Eur. J. Org. Chem.* **2015**, *2015*, 5944–5948.

- (7) de Bellefon, C.; Fouilloux, P. Homogeneous and Heterogeneous Hydrogenation of Nitriles in a Liquid Phase: Chemical, Mechanistic and Catalytic Aspects. *Catal. Rev.: Sci. Eng.* **1994**, *36* (3), 459–506.
- (8) Lévay, K.; Hegedűs, L. Selective Hydrogenation of Nitriles to Primary Amines. *Period. Polytech., Chem. Eng.* **2018**, *62* (4), 476–488.
- (9) Rylander, P. N. *Catalytic Hydrogenation over Platinum Metals*; Academic Press: New York, 1967.
- (10) Freifelder, M. *Practical Catalytic Hydrogenation: Techniques and Applications*; Wiley: New York, 1971.
- (11) Krupka, J.; Pašek, J. Nitrile Hydrogenation on Solid Catalysts—New Insights into the Reaction Mechanism. *Curr. Org. Chem.* **2012**, *16* (8), 988–1004.
- (12) Volf, J.; Pašek, J. Chapter 4 Hydrogenation of Nitriles. *Stud. Surf. Sci. Catal.* **1986**, *27*, 105–144.
- (13) Greenfield, H. Catalytic Hydrogenation of Butyronitrile. *Ind. Eng. Chem. Prod. Res. Dev.* **1967**, *6* (2), 142–144.
- (14) Vilches-Herrera, M.; Werkmeister, S.; Junge, K.; Börner, A.; Beller, M. Catalytic transfer hydrogenation of nitriles to primary amines using Pd/C. *Catal. Sci. Technol.* **2014**, *4*, 629–632.
- (15) McAllister, M. I.; Boulho, C.; McMillan, L.; Gilpin, L. F.; Brennan, C.; Lennon, D. The hydrogenation of mandelonitrile over a Pd/C catalyst: towards a mechanistic understanding. *RSC Adv.* **2019**, *9*, 26116–26125.
- (16) McAllister, M. I.; Boulho, C.; Brennan, C.; Sidebottom, P. J.; Lennon, D. Isotopic substitution experiments of mandelonitrile over a carbon supported Pd catalyst: A nuclear magnetic resonance study. *Mol. Catal.* **2020**, *484*, 110720.
- (17) McAllister, M. I.; Boulho, C.; McMillan, L.; Gilpin, L. F.; Wiedbrauk, S.; Brennan, C.; Lennon, D. The production of tyramine via the selective hydrogenation of 4-hydroxybenzylcyanide over a carbon-supported palladium catalyst. *RSC Adv.* **2018**, *8*, 29392–29399.
- (18) Hegedűs, L.; Máthé, T.; Kárpáti, T. Selective heterogeneous catalytic hydrogenation of nitriles to primary amines in liquid phase Part II: Hydrogenation of benzyl cyanide over palladium. *Appl. Catal., A* **2008**, *349*, 40–45.
- (19) Marella, R. K.; Koppadi, K. S.; Jyothi, Y.; Rama Rao, K. S.; Burri, R. B. Selective gas-phase hydrogenation of benzonitrile into benzylamine over Cu–MgO catalysts without using any additives. *New J. Chem.* **2013**, *37*, 3229–3235.
- (20) Chatterjee, M.; Kawanami, H.; Sato, M.; Ishizaka, T.; Yokoyama, T.; Suzuki, T. Hydrogenation of nitrile in supercritical carbon dioxide: a tunable approach to amine selectivity. *Green Chem.* **2010**, *12*, 87–93.
- (21) Huang, Y.; Sachtler, W. M. H. Catalytic Hydrogenation of Nitriles over Supported Mono- and Bimetallic Catalysts. *J. Catal.* **1999**, *188*, 215–225.
- (22) Parker, S. F.; Lennon, D.; Albers, P. W. Vibrational Spectroscopy with Neutrons: A Review of New Directions. *Appl. Spectrosc.* **2011**, *65* (12), 1325–1341.
- (23) Tamas, A.; Martagiu, R.; Minea, R. Experimental Determination of Mass Transfer Coefficients in Dissolution Processes. *Chem. Bull.* **2007**, *52* (66), 133–138.
- (24) Fernando, W. J. N.; Othman, M. R.; Karunaratne, D. G. G. P. Agitation Speed and Interfacial Mass Transfer Coefficients in Mass Transfer Dominated Reactions. *Int. J. Eng. Technol.* **2011**, *11* (01), 71–79.
- (25) Dietrich, E.; Mathieu, C.; Delmas, H.; Jenck, J. Raney Nickel-Catalysed Hydrogenations: Gas-Liquid Mass Transfer in Gas-Induced Stirred Slurry Reactors. *Chem. Eng. Sci.* **1992**, *47* (13–14), 3597–3604.
- (26) Nasirzadeh, K.; Zimin, D.; Neueder, R.; Kunz, W. Vapor-Pressure Measurements of Liquid Solutions at Different Temperatures: Apparatus for Use over an Extended Temperature Range and Some New Data. *J. Chem. Eng. Data* **2004**, *49*, 607–612.
- (27) Suwardiyanto; Howe, R. F.; Gibson, E. K.; Catlow, R. C.; Hameed, A.; McGregor, J.; Collier, P.; Parker, S. F.; Lennon, D. An assessment of hydrocarbon species in the methanol-to-hydrocarbon reaction over a ZSM-5 catalyst. *Faraday Discuss.* **2017**, *197*, 447–471.

(28) Mitchell, P. C. H.; Parker, S. F.; Ramirez-Cuesta, A. J.; Tomkinson, J. *Vibrational Spectroscopy with Neutrons, with Applications in Chemistry, Biology, Materials Science and Catalysis*; Series on Neutron Techniques and Applications, Vol. 3; World Scientific: Singapore, 2005.

(29) Parker, S. F.; Lennon, D.; Albers, P. W. Vibrational Spectroscopy with Neutrons – New Directions. *Appl. Spectrosc.* **2011**, *65*, 1325–1341.

(30) Augustine, R. L. *Heterogeneous Catalysis for the Synthetic Chemist*; Marcel Dekker: New York, 1996.

(31) Stamatiou, I. K.; Muller, F. L. Determination of mass transfer resistances in trickle bed reactors. *Chem. Eng. J.* **2019**, *377*, 119808.

(32) Perego, C.; Pertello, S. Experimental methods in catalytic kinetics. *Catal. Today* **1999**, *52*, 133–145.

(33) Machado, R. M. Fundamentals of Mass Transfer and Kinetics for the Hydrogenation of Nitrobenzene to Aniline. *ARL Application Note* **2007**, *1*, 1–13.

(34) Dai, C.; Zhu, S.; Wang, X.; Zhang, C.; Zhang, W.; Li, Y.; Ning, C. Efficient and selective hydrogenation of benzonitrile to benzylamine: improvement on catalytic performance and stability in a trickle-bed reactor. *New J. Chem.* **2017**, *41*, 3758–3765.

(35) Arai, M.; Takada, Y.; Nishiyama, Y. Effects of Metal Particle Size in Gas-Phase Hydrogenation of Acetonitrile over Silica-Supported Platinum Catalysts. *J. Phys. Chem. B* **1998**, *102*, 1968–1973.

(36) Kulkarni, A.; Zhou, W.; Török, B. Heterogeneous catalytic hydrogenation of unprotected indoles in water: A green solution to a long standing challenge. *Org. Lett.* **2011**, *13* (19), 5124–5127.

(37) Albers, P.; Pietsch, J.; Parker, S. F. Poisoning and deactivation of palladium catalysts. *J. Mol. Catal. A: Chem.* **2001**, *173*, 275–286.

(38) Hamilton, N. G.; Silverwood, I. P.; Warringham, R.; Kapitán, J.; Hecht, L.; Webb, P. B.; Tooze, R. P.; Parker, S. F.; Lennon, D. Vibrational Analysis of an Industrial Fe-Based Fischer–Tropsch Catalyst Employing Inelastic Neutron Scattering. *Angew. Chem., Int. Ed.* **2013**, *52*, 5608–5611.

(39) Lin-Vien, D.; Colthup, N. B.; Fateley, W. G.; Grasselli, J. G. *The Handbook of Infrared and Raman Characteristic Frequencies of Organic Molecules*; Academic Press, 1991.

(40) Silverwood, I. P.; Hamilton, N. G.; Laycock, C. J.; Staniforth, J. Z.; Ormerod, R. M.; Frost, C. D.; Parker, S. F.; Lennon, D. Quantification of surface species present on a nickel/alumina methane reforming catalyst. *Phys. Chem. Chem. Phys.* **2010**, *12*, 3102–3107.